

# **A Standardized Procedure for Analysis of the Dynamic Modulus ( $|E^*|$ ) Data to Predict Asphalt Pavement Distresses**

**Aroon Shenoy**

*Senior Research Fellow*

*Turner-Fairbank Highway Research Center*

*6300 Georgetown Pike*

*McLean, VA 22101*

*Tel: 202-493-3105; Fax: 202-493-3161; e-mail: aroon.shenoy@fhwa.dot.gov*

and

**Pedro Romero**

*Assistant Professor*

*Department of Civil and Environmental Engineering*

*The University of Utah*

*Salt Lake City, UT 84112*

*Tel: 801-587-7725; Fax: 801-585-5477; e-mail: romero@eng.utah.edu*

*Word Count:       Text = 4509*

*8 Tables = 2000*

*5 Figures = 1250*

-----  
*Total = 7759*

## Abstract

*The present work provides a standardized procedure by which various asphalt concrete mixtures can be compared and their expected performance can be assessed in a uniform manner using the simple performance test suggested under the National Co-operative Highway Research Program NCHRP 9-19 – Superpave Support and Performance Models Management program.*

*The frequency sweep data generated from the test are available in terms of dynamic modulus  $|E^*|$  versus frequency at the measurement temperature under different levels of confining stress (0, 20, 30 psi or 0, 2.9, 4.35 mPa). The moduli versus frequency data at different temperatures are unified to form a single curve for each mixture through a normalizing parameter. The temperature at which the normalizing parameter becomes equal to one is designated the specification parameter  $T_S$  ( $^{\circ}\text{C}$ ) for assessing mixture performance.*

*Each unified curve is fitted with a constitutive equation from which model parameters are evaluated. The slope  $B_1$  in the low frequency region of the unified curve, when normalized with the term  $(T/T_S)$ , results in a parameter that is related to asphalt pavement distress at high temperature  $T$ . It is shown that  $B_1/T_S$  is related to rut depths measured at different WesTrack, a full-scale test track, sections and the correlation improves with increasing confining stress. There is a good possibility that the slope  $B_2$  in the high frequency region of the unified curve may relate to distresses in the intermediate temperature range, such as fatigue cracking. A preliminary check shows that this might be true, but data is too limited to draw firm conclusions.*

**Keywords:** *Simple performance test, frequency sweep, standardized procedure, performance-related specifications, aggregate-asphalt combinations, mixture evaluation*

---

## Introduction

A Simple Performance Test to estimate intermediate and high temperature distresses of asphalt mixtures is being evaluated under the Superpave Models Management Contract Task C – Simple Performance Study (1). The triaxial complex modulus test used in this study involves the application of a sinusoidal strain with a certain peak amplitude under different levels of confining stress (0, 20, 30 psi or 0, 2.9, 4.35 mPa) at a fixed temperature of interest at each of the following frequencies: 25, 10, 5, 2, 1, 0.5, and 0.1 Hz. The response of the material at these frequencies to the applied strain is analyzed in terms of the complex modulus ( $E^*$ ) and the phase angle ( $\phi$ ). The aim of the study was (1) to measure the stiffness characteristics of ten mixtures from WesTrack, a full-scale test track (2-4) and (2) to relate the absolute value of the complex modulus, termed the dynamic modulus  $|E^*|$ , obtained from servo-hydraulic testing to the distresses in the pavement at intermediate and high temperatures.

The relationship is established under the hypothesis that the stiffness of the asphalt mixture can be used to predict distresses at intermediate and high temperatures. Stiffness using the dynamic modulus test is the parameter of choice for the National Co-operative Highway Research Program NCHRP 9-19 – Superpave Support and Models contract as well as the

American Association of State Highway and Transportation Officials AASHTO 2002 design guide (5). The stiffer the mixture at high temperatures, the more rut resistant the mixture is expected to be in the field. At intermediate temperatures, the stiffer mixture is more resistant to fatigue cracking for thicker pavements while the softer mixture is more resistant to fatigue cracking for thinner pavements.

Using properties measured on laboratory-prepared mixtures and from field performance data on ten sections of the WesTrack, a full-scale test track (2-4) test site, the measured stiffness of the mixtures is compared to the equivalent measured rut depth and cracking ( $I$ ). For rutting, the analysis ( $I$ ) was conducted for two combinations of temperature [100°F (37.8°C), 130°F (54.4°C)] and one time of loading [5 Hz]. For fatigue cracking, the analysis ( $I$ ) was conducted for different two combinations of temperature [40°F (4.4°C), 70°F (21.1°C)] and a different time of loading [10 Hz].

The choice of their combinations of temperatures and loading time for each of the distresses is, undoubtedly, appropriate because rutting is expected to occur at higher temperatures and lower loading times while fatigue cracking is expected to occur in the lower range of temperatures and higher loading times. However, neither the temperatures nor the times of loading are selected on any standardized basis. Hence, different researchers could choose different values of temperatures and loading times as per their own convenience or preference so long as they relate the higher temperatures and lower loading times to rutting behavior, and the lower temperatures and higher loading times to fatigue behavior. This could result in different researchers coming up with different conclusions when comparing the same set of mixtures if their temperature and loading time choices are different. Such a practice will eventually lead to the availability of lots of mixture data that, however, cannot be compared on a common platform. Thus, the information from the simple performance test will be under-utilized and restricted to only specific systems under the limited sets of chosen test conditions.

The present paper establishes a standardized procedure to analyze and interpret data generated from the triaxial test proposed in the NCHRP 9-19 program ( $I$ ). This is done by reanalysis of data already generated under the NCHRP 9-19 program ( $I$ ). The set up procedure is general in nature. There are no restrictions on the choice of the temperatures of measurement. Any temperatures within the range of low temperature [e.g. 15.8°F (-9°C)] and high temperature [e.g. 130°F (54.4°C)] may be chosen in order to generate a specification temperature  $T_s$ . Using a normalizing parameter, a unified curve is generated within a temperature range, which again is insensitive to the actual choice of the temperatures. So long as three temperatures are selected between the intermediate temperature [e.g. 40°F (4.4°C)] and high temperature [e.g. 100°F (40°C)], the unified curve generated by the suggested procedure will be the same for the same mixture.

The unified curve is then fitted with a rheological model, and the values of the model parameters are determined. The slopes  $B_1$  and  $B_2$  in the low frequency and high frequency portions of the unified curve are used for determining the controlling terms  $C_R$  and  $C_F$  for ranking the aggregate-asphalt mixtures by their expected performance to resist distresses in high and intermediate temperature ranges. The assessment parameters ( $T_s$ ,  $C_R$ , and  $C_F$ ) introduced in the present work could be used as identification tags to grade mixtures and rank their expected field performance. This would then establish uniformity among different researchers and data sharing

between various practitioners would occur on a common platform. It would also be useful for developing mixtures targeted towards particular specifications when designing pavements for specific regions.

### Mixture Compositions

The mixtures analyzed in the present work are those described in detail in the NCHRP report (1). The specimens were fabricated in the laboratory to duplicate the measured material compositions for each of the ten WesTrack test sections utilized in the study, namely, sections 2, 4, 7, 15, 23 and 24 for rutting and sections 2, 5, 6 and 24 for cracking. Table 1 gives the binder and air void content as well as gradations for the mixtures, and Table 2 gives the measured rut depths and fatigue cracking as percent area.

### Sample Preparation

All mixtures were designed using the SHRP level 1 (Volumetric) mix design method with one conventional PG64-22 binder. The mixing and compaction temperatures were determined using the protocol followed earlier by the NCHRP 9-19 research team (6).

All mixtures were short-term oven aged for 4 hours at 135°C according to the AASHTO test method (7) before compaction. The specimens were compacted with a 'Servo Pac Gyratory Compactor' into a 150-mm diameter gyratory mold to approximately 160-mm height. Test samples of 100-mm diameter were cored from the center of the gyratory compacted specimen. Approximately 5 mm were sawed from each sample end in accordance with the NCHRP 9-19 research team's protocol (6).

### Specification Temperature $T_s$ (°C)

The procedure to obtain a specification temperature follows along the lines introduced earlier (8, 9) during the analysis of the frequency sweep at constant height (FSCH) data generated from the Superpave Shear Tester (SST).

The triaxial complex modulus testing data is available in the form of the variation of the dynamic modulus  $|E^*|$  with frequency  $\omega$  at five different temperatures, namely, 15.8°F (-9°C), 40°F (4.4°C), 70°F (21.1°C), 100°F (37.8°C) and 130°F (54.4°C). A normalizing frequency parameter  $\omega_0$  is first determined corresponding to a particular reference dynamic modulus value. The choice of the reference dynamic modulus is arbitrary as has been explained in previous publications (8, 9). In the present case, the reference dynamic modulus  $|E_0^*|$  value is chosen to be equal to 4,000,000 Pa, and this value is recommended for future data analyses. The value of  $\omega_0$  corresponding to the reference dynamic modulus  $|E_0^*| = 4,000,000$  Pa is estimated using the following equation:

$$\ln \omega_0 = \ln \omega_1 + \ln \left( \frac{\omega_1}{\omega_2} \right) * \left( \frac{\ln \frac{|E_0^*|}{|E_1^*|}}{\ln \frac{|E_1^*|}{|E_2^*|}} \right) \text{----- (1)}$$

where the normalizing frequency parameter  $\omega_0$  corresponds to the reference dynamic modulus  $|E_0^*|=4,000,000$  Pa.  $|E_1^*|, \omega_1$  and  $|E_2^*|, \omega_2$  are two sets of data corresponding to (a) one value of  $|E^*| > 4,000,000$  Pa and (b) another value of  $|E^*| < 4,000,000$  Pa. In cases where data does not include the range covering the value of  $|E_0^*|=4,000,000$  Pa, Equation (1) is used for extrapolation. The values of  $\omega_0$  for various mixtures are given in Table 3.

The variation of the normalizing frequency parameter with temperature is expressed through a semi-logarithmic plot of  $\omega_0$  versus  $1/T$  (where  $T$  is the temperature in degrees Kelvin) (8, 9). The data points are fitted with the best line ( $R^2 \approx 0.93-0.97$ ) using an equation of the following form (8, 9):

$$\omega_0 = \exp\left(A_0\left(1 - \frac{T_0}{T}\right)\right) \text{-----} (2)$$

The values of  $A_0$  and  $T_0$  for all sets of data as determined from Equation (2) are given in Table 4. The specification temperature is determined as  $T_S$  ( $^{\circ}\text{C}$ ) =  $T_0$  (K) - 273. This is in essence the temperature at which the mixture has a stiffness of 4,000,000 Pa at a loading frequency of 1 Hz.

Using the appropriate value of  $\omega_0$  corresponding to each temperature, the original data of  $|E^*|$  versus  $\omega$  as shown in Figure 1 (for one mixture sample) are replotted as  $|E^*|$  versus  $\omega / \omega_0$  in Figure 2 combining data for the different temperatures, basically using the principles of time-temperature superposition. It can be seen that a unified curve is obtained through the use of this normalization. Only three temperatures [40 $^{\circ}$ F (4.4 $^{\circ}$ C), 70 $^{\circ}$ F (21.1 $^{\circ}$ C), 100 $^{\circ}$ F (37.8 $^{\circ}$ C)] are utilized in the unification for the following reasons. First, the lowest temperature of 15.8 $^{\circ}$ F (-9 $^{\circ}$ C) and the highest temperature of 130 $^{\circ}$ F (54.4 $^{\circ}$ C) include data wherein the values of  $\omega_0$  were obtained by gross extrapolation and, hence, would not give reliable unification. Second, the three temperatures [40 $^{\circ}$ F (4.4 $^{\circ}$ C), 70 $^{\circ}$ F (21.1 $^{\circ}$ C), 100 $^{\circ}$ F (37.8 $^{\circ}$ C)] suffice to cover the temperature range from intermediate to high that is relevant to the distresses of fatigue cracking and rutting, because the unification automatically extends the range beyond the values of 40 $^{\circ}$ F (4.4 $^{\circ}$ C) and 100 $^{\circ}$ F (37.8 $^{\circ}$ C) based on the superposition principle. Unified curves similar to the one shown in Figure 2 were obtained for all mixture data sets in Table 3.

The best-fit curves through the data points in Figure 2 and other similar unified curves (not shown here) are obtained using the following equation having a form similar to the one used in the earlier work for fitting unified curves for (a) mixtures from the SST data [8, 9] and (b) asphalt binders from dynamic shear rheometer (DSR) data [10]:

$$|E^*| = \left( \frac{A_1(\omega / \omega_0)^{B_1}}{[1 + \{(A_1 / A_2)^{2/(B_1-B_2)}(\omega / \omega_0)^2\}]^{(B_1-B_2)/2}} \right) \text{-----} (3)$$

where the values of  $A_1, B_1, A_2$  and  $B_2$  for the unified curve for each mixture are given in Table 5.

The development of the unified curves in the manner described herein has a number of distinct advantages. The unified curve helps to extend the range of data and can be used for predicting the dynamic mechanical behavior of the mixture at temperatures outside the measured values. For example, though the temperatures used for the unification are 40°F (4.4°C), 70°F (21.1°C) and 100°F (37.8°C), the values of  $\omega_0$  at temperatures outside this range can be predicted using Equation (2) and values of  $A_0$  and  $T_0$  from Table 4. These values of  $\omega_0$ , in turn, when used in Equation (3) with values of coefficients  $A_1$ ,  $A_2$  and exponents  $B_1$ ,  $B_2$  from Table 5 help to give the variation of  $|E^*|$  versus  $\omega$  at any other temperature of interest. This fact becomes useful, especially, when there is a need to know the dynamic mechanical behavior of the mixture at a temperature where the sample stiffness, particularly of a low performance grade binder, makes the measurement fall outside the sensitive range of the equipment.

The model described by Equation (3) that is used for fitting the data points on the unified curve is a combination of the following two equations – one for the lower frequency region and the other for the higher frequency region (8-10):

$$|E^*| = A_1(\omega / \omega_0)^{B_1} \text{ for } 0.00001 < \omega/\omega_0 < 1 \quad \text{-----(4a)}$$

$$|E^*| = A_2(\omega / \omega_0)^{B_2} \text{ for } 1 < \omega/\omega_0 < 100000 \quad \text{-----(4b)}$$

This automatically marks the two portions of the unified curve that are of significance. The portion of the unified curve in the low frequency region describes the dynamic mechanical behavior of the mixture at higher temperatures applicable to rutting, while the other portion of the unified curve in the higher frequency region describes the dynamic mechanical behavior at lower temperatures applicable to the intermediate temperature distress of fatigue cracking. This is because the unification automatically aligns data at higher temperatures so as to lie in the lower region of the normalized frequency while aligning data at intermediate temperatures to fall within the higher region of normalized frequency.

Thus, an indicator of mixture resistance to permanent deformation at high temperatures should, in principle, be linked to the portion of the unified curve in the lower frequency region given by Equation (4a). The stiffness of the mixture at the temperature of interest could be obtained from this equation at any desired frequency or frequencies. If a single frequency value is used, then the dynamic mechanical behavior is expressed at one specific condition only. The coefficient  $A_1$  is actually the value of stiffness at  $\omega/\omega_0 = 1$  and is again an expression of the dynamic mechanical behavior under one specific condition. On the other hand, the exponent  $B_1$ , being the slope of  $|E^*|$  versus  $\omega/\omega_0$  on a log-log plot, captures the behavioral pattern through a range of temperatures and frequencies applicable to rutting. Hence,  $B_1$  is recommended for use in order to establish the relationship between the dynamic mechanical data and rutting.

The lower the exponent  $B_1$ , the greater is the resistance of the mixture to rutting. Similarly, the higher the value of  $T_S$ , the greater is the resistance of the mixture to rutting. This implies that the permanent deformation  $D_T$  at temperature  $T$  would essentially be a function of  $T$ ,  $T_S$  and  $B_1$ . The form  $(T/T_S)^{B_1}$  would give an adequate description of this function and could be

considered as the rutting control term,  $C_R$ , for giving a measure of the rutting resistance. The lower the value of  $C_R$ , the better is the rutting resistance. The rutting control term  $C_R$  is given by the following equation:

$$C_R = (T / T_S) B_1 \text{-----} (5)$$

If the temperature of interest  $T$  were equal to the specification temperature  $T_S$ , then the rutting control term  $C_R$  would simply be equal to  $B_1$ . Thus, in such circumstances, if one were to compare the behavior of two mixtures at their respective specification temperatures, then it would be sufficient to compare their respective  $B_1$  values to ascertain that the one with the lower value would be expected to exhibit less rutting under the same loading and environmental conditions.

On the other hand, if the temperature of interest were a particular average pavement temperature  $T$ , then to understand how two mixtures would perform under identical temperature conditions, it would be enough to compare their  $(B_1 / T_S)$  ratio. As a matter of fact, it would be this ratio that could be used for ranking mixtures.

Table 6 gives the values of the  $(B_1 / T_S)$  ratio for the mixtures analyzed in this work. The lab-predicted permanent deformation based on the  $(B_1 / T_S)$  ratio when compared with the field rut depth shows the correlation for the WesTrack sections in Figures 3-5 for different confining stresses of 0, 20, 30 psi (0, 2.9, 4.35 mPa), respectively. The correlation coefficient  $R^2$  is 0.42 when data is acquired from tests performed under unconfined conditions. The correlation coefficient  $R^2$  improves to 0.60 when confining stress of 20 psi (2.9 mPa) is used during data acquisition. It is known that confined creep testing in triaxial measurements has a better correlation to permanent deformation than unconfined testing [11]. Thus, when a higher confining stress of 30 psi (4.35 mPa) is used in the measurements, the correlation coefficient  $R^2$  rises to 0.89, indicating that these conditions favor a good correlation between the laboratory test and field performance. The confining stress in the WesTrack pavements based on truck loadings is not known. However, the present work indicates that the suggested method of using the slope of the unified curve obtained from data when confining stress equals 30 psi (4.35 mPa) is effective in predicting mixture rutting performance. It is therefore recommended for future use with an understanding that this is not the optimum value, and a value greater than 30 psi (4.35 mPa), perhaps 40 psi (5.8 mPa), may be an optimum and should be used if such a value is determined through future experiments.

The portion of the unified curve in the higher frequency region describes the dynamic mechanical behavior at lower temperatures applicable to the other distress mode, namely, fatigue cracking. The exponent representing the behavior in that portion of the curve is  $B_2$ . The structural design of the pavement would dictate whether a higher stiffness material or a lower stiffness material would mitigate this distress at intermediate temperatures. As an example, a pavement structure wherein a material with lower stiffness would provide better resistance to fatigue cracking could be considered. In such a circumstance, the resistance of the mixture to the distress at intermediate temperatures would be greater when the exponent  $B_2$  is lower and the value of  $T_S$  is lower. This implies that the resistance to intermediate temperature distress at temperature  $T$  would adequately be described by the functional form  $(T_S / T)^* B_2$  and this could be

considered as the control term  $C_F$ , giving a measure of the resistance of a mixture to the intermediate temperature distress of fatigue cracking. The lower the value of  $C_F$ , the better would be the resistance.

The control term  $C_F$  would simply be equal to  $B_2$  in case the temperature of interest were equal to the specification temperature. Thus, in such circumstances, if one were to compare the behavior of two mixtures at their respective specification temperatures, then it would be sufficient to compare their respective  $B_2$  values to ascertain that the one with the lower value would be expected to exhibit less fatigue cracking at intermediate temperatures.

On the other hand, if the temperature of interest were a particular average pavement temperature  $T$ , then it would be enough to compare their  $(T_S * B_2)$  product in order to evaluate how two mixtures would perform under identical temperature conditions, and in fact, this product could be used for ranking mixtures.

Table 7 gives the values of the  $(T_S * B_2)$  product for the mixtures analyzed in this work. A comparison with field performance cannot be done in an effective manner because the field information on cracking is available for only three sites. When plots of  $T_S * B_2$  were made against the cracking length for the three sections, the correlation coefficient  $R^2 = 0.8$  was obtained for a confining stress of 30 psi (4.35 mPa). However, much emphasis should not be placed on this result as it was obtained with only three data points, and the findings from this part of the analysis should be reconfirmed when more data becomes available.

### Concluding Remarks

The present work introduces certain assessment parameters ( $T_S$ ,  $C_R$ , and  $C_F$ ) that could be used as identification tags to grade mixtures and rank their expected field performance. This method of performance-related specification would help in streamlining the data analysis procedure from triaxial modulus testing. It would provide a uniform platform to compare data from different practitioners and project the expected performance of the mixtures. It would also be useful for developing mixtures targeted towards particular specifications when designing pavements for specific regions.

The suggested method is simple and straightforward. It involves the determination of a specification temperature  $T_S$  ( $^{\circ}\text{C}$ ) from the dynamic modulus versus frequency data. This is done by determining the normalizing parameter  $\omega_0$  corresponding to the value of  $|E_0^*| = 4,000,000$  Pa using Equation (1). The values of  $\omega_0$  at two different temperatures are sufficient to determine the value of  $T_0$  (K) from Equation (2), from which  $T_S$  ( $^{\circ}\text{C}$ ) is immediately obtained. In case  $\omega_0$  is available at more than two temperatures (as was the case in the present work), then a semi-logarithmic plot of  $\omega_0$  versus  $1/T$  (K) is to be used to determine the value of  $T_0$  (K) and, subsequently,  $T_S$  ( $^{\circ}\text{C}$ ).

The dynamic modulus  $|E^*|$  versus frequency  $\omega$  data at different temperatures for each aggregate-asphalt mixture is unified by normalizing the frequency using corresponding values of  $\omega_0$ . The unified data is then fitted with the rheological model given by Equation (3), and the values of the model parameters are determined. The slopes  $B_1$  and  $B_2$  of the two portions of the unified curve are used for determining the controlling terms  $C_R$  and  $C_F$  for ranking the aggregate-asphalt mixtures by their expected performance to resist distresses in high and intermediate

The reliability of the information generated from the slopes  $B_1$  and  $B_2$  is dependent on the quality of the generated data and the resultant unification. The experimental data must be generated within the sensitive range of the equipment capabilities. In order to ensure that this is always the case, it is prudent to generate dynamic modulus versus frequency data in the triaxial modulus test for different binders not at some predetermined fixed temperatures but rather at temperatures where the stiffness of the material is within the measurement sensitivity of the equipment. For example, it would be better to take data at lower temperatures from 5°C to 30°C for low stiffness binders while at higher temperatures from 15°C to 40°C for high stiffness binders. This would result in data that will unify without scatter over the entire frequency range.

By generating data within different temperatures but similar stiffness ranges, the other advantage is that the normalizing parameter will not need gross extrapolation. Using unextrapolated values of  $\omega_0$  would result in better unification of data. It is difficult to guess the stiffness of the aggregate-asphalt system before any triaxial modulus measurements are performed. Hence, it may not always be easy to choose the temperature range for the measurement such that the stiffness of the system lies within the sensitivity range of the equipment.

Based on the present work, a rough guideline is suggested that should help in making a reasonable choice of the measurement temperatures. It is recommended that the first measurement temperature should be chosen to be half the value of the high performance grade temperature of the binder used. The subsequent temperatures are selected such that each is lower by 6°C. Table 8 shows an example of how the temperatures could be chosen.

It should be noted that the methodology described herein only addresses load-related distresses. In addition, the case of thick pavements where stiff mixtures are desired for resistance to fatigue cracking was not considered in the analysis. The controlling term for this case can be easily deduced because the functional form must be the same as that for the rutting control term, except for the fact that  $B_1$  needs to be replaced by  $B_2$ . A higher value of  $B_2$  and a lower value of  $T_S$  would indicate better resistance of thick pavements to fatigue cracking. Thus, for the case of thick pavements, the control term for fatigue cracking  $C_F = (T/T_S) * B_2$ , and higher the  $C_F$  value the better would be the resistance of such pavements to fatigue cracking.

The concepts used in this work are general in nature and applicable to mixtures as well as binders [8-10]. The developed methodology in principle should be applicable to any pavement. Thus, it is recommended that this analysis procedure be checked with data from other test sites and with other unmodified and modified binders in order to validate the findings of this work.

## **Disclaimer**

The opinions, findings, and conclusions expressed in this document are those of the authors only and not necessarily of the Federal Highway Administration or the University of Utah.

## **Acknowledgements**

The authors would like to express their gratitude to Dr. Ernest J. Bastian, Jr. for his comments.

## References

1. Witczak, M. W. and T. K. Pellinen. *Superpave Support and Performance Models Management, NCHRP 9-19, Task C – Simple Performance Test, WesTrack Experimental Site*. Team Report SPT-WST-2 (J-K), July 2000.
2. Mitchell, T. M. WesTrack: The Road to Solutions, *Public Roads*, Vol. 60, No. 2, autumn, 1996.
3. FHWA Report, *WesTrack: Performance Testing for Quality Roads*, Publication No. FHWA-SA-97-038, 1997.
4. Nevada Automotive Test Center. WesTrack: Project Description. [www.westrack.com/wt\\_01.htm](http://www.westrack.com/wt_01.htm), 1997.
5. Harman, T. Using the Dynamic Modulus Test to Assess the Mix Strength of HMA, *Public Roads*, May/June 2001, pp. 6-8.
6. Kaloush, K. and M. W. Witczak. *In-Situ Mixture Composition and Performance Data for the WesTrack Mixtures*. Team Report SPT-WST-1, Arizona State Univ., February 2000.
7. AASHTO Test Method PP2. *Standard Practice for Short and Long Term Aging of Hot Mix Asphalt*.
8. Shenoy, A. and P. Romero. Determining a Specification Parameter for Asphalt Mixtures using Unified Frequency Sweep at Constant Height Data from the Superpave Shear Tester. *International Journal of Road Materials and Pavement Design*, Vol. 1, No. 1, 2000, pp. 75-96.
9. Shenoy, A. and P. Romero. Superpave Shear Tester as a Simple Standardized Measure to Evaluate Aggregate-Asphalt Mixture Performance. *ASTM – Journal of Testing & Evaluation*, Vol. 29, No. 5, Sept. 2001, pp. 50-62.
10. Shenoy, A. Model-fitting the Master Curves of the Dynamic Shear Rheometer Data to Extract a Rut-Controlling Term for Asphalt Pavements. *ASTM – Journal of Testing & Evaluation*, Vol. 30, No. 2, March 2002.
11. Roberts, F. L., Kandhal, P. S., Brown, E. R., Lee, D. Y. and T. W. Kennedy. *Hot Mix Asphalt Materials, Mixture Design, and Construction*. National Asphalt Pavement Association Education Foundation, Lanham, Maryland, 1991.

## List of Tables

**TABLE 1 – WesTrack Mixture Compositions (1)**

**TABLE 2 – WesTrack Performance Data (1)**

**TABLE 3 – Values of the normalizing frequency parameter,  $\omega_0$  (Hz) using  $|E^*_0|=4,000,000(\text{Pa})$**

**TABLE 4 – Values of  $A_0$ ,  $T_0(\text{K})$  and  $T_S(^{\circ}\text{C})$  from Equation (2)**

**TABLE 5 – Values of the coefficients and exponents in Equation (3)**

**TABLE 6 – Performance ranking for resistance to distress at high temperatures**

**TABLE 7 – Performance ranking for resistance to distress at intermediate temperatures**

**TABLE 8 – Examples of proper choice of temperatures for triaxial modulus testing**

**List of Figures**

**Figure 1:** *Dynamic modulus  $|E^*|$  with frequency  $\omega$  at three different temperatures of 40°F (4.4°C), 70°F (21.1°C), and 100°F (37.8°C) for WST\_WC2 laboratory-prepared samples*

**Figure 2:** *Unified curve of the dynamic modulus  $|E^*|$  with modified frequency  $\omega / \omega_0$  covering a range of 40°F (4.4°C) - 100°F (37.8°C) for WST\_WC2 laboratory-prepared samples*

**Figure 3:** *Variation of the term  $(B_1/T_S)$  obtained from the triaxial modulus unconfined (confining stress=0psi or 0mPa) testing of laboratory-prepared samples with rut depth measurements (in millimeters) from field performance*

**Figure 4:** *Variation of the term  $(B_1/T_S)$  obtained from the triaxial modulus (confining stress=20psi or 2.9mPa) testing of laboratory-prepared samples with rut depth measurements (in millimeters) from field performance*

**Figure 5:** *Variation of the term  $(B_1/T_S)$  obtained from the triaxial modulus (confining stress=30psi or 4.35mPa) testing of laboratory-prepared samples with rut depth measurements (in millimeters) from field performance*

**TABLE 1 –WesTrack Mixture Compositions (I)****(a) Volumetric Properties**

<b>Section</b>	<b>Aggregate Nominal Size (mm)</b>	<b>Binder Type</b>	<b>AC %</b>	<b>V<sub>a</sub> %</b>	<b>G<sub>mm</sub></b>	<b>Distress: C=Cracking R=Rutting</b>
2	12.5 Fine-B	PG 64-22	4.76	9.3	2.466	C
24	12.5 Coarse-B	PG 64-22	5.78	7.5	2.431	C
5	12.5 Fine-B	PG 64-22	5.61	7.0	2.437	C
6	12.5 Fine-B	PG 64-22	5.89	11.3	2.427	C
15	12.5 Fine-T	PG 64-22	5.55	8.7	2.438	R
2	12.5 Fine-T	PG 64-22	5.02	10.4	2.457	R
23	12.5 Coarse-T	PG 64-22	5.78	4.9	2.430	R
24	12.5 Coarse-T	PG 64-22	5.91	7.2	2.425	R
4	12.5 Fine-T	PG 64-22	5.24	6.6	2.449	R
7	12.5 Coarse-T	PG 64-22	6.28	6.9	2.412	R

B=Bottom layer; T=Top layer

**(b) Gradations**

<b>Sieve mm</b>	<b>Fine</b>		<b>Coarse</b>	
	<b>Top % Passing</b>	<b>Bottom % Passing</b>	<b>Top % Passing</b>	<b>Bottom % Passing</b>
19.0	100	100	100	100
12.5	88.2	88.3	79.2	81.7
9.50	76.6	75.9	65.0	66.2
4.75	51.1	48.6	41.8	42.0
2.36	39.8	36.7	28.6	27.7
1.18	35.2	32.3	21.0	19.9
0.60	28.6	26.4	16.1	14.9
0.30	16.1	15.1	12.2	11.0
0.15	8.1	7.4	9.0	7.9
0.075	5.0	4.4	6.6	5.5

**TABLE 2 – WesTrack Performance Data (I)**

<b>Section</b>	<b>Gradation</b>	<b>% Cracking =100*crack length/section length</b>	<b>Rut Depth millimeters</b>
(a) Cracking Sections measured on 5/27/1997 at 2.8M ESALs			
2	Fine	7	6
24	Coarse	0	22
5	Fine	51	-
6	Fine	100	21
(b) Rutting Sections measured on 11/11/1997 at 1.5M ESALs			
15	Fine	0	8
2	Fine	7	6
23	Coarse	-	13
24	Coarse	0	22
4	Fine	-	7
7	Coarse	-	36

**TABLE 3 -- Values of the normalizing frequency parameter,  $\omega_0$  (Hz) using  $|E^*_0|=4,000,000(\text{Pa})$** 

Mixture	$\omega_0$				
	@15.8°F (-9°C)	@40°F (4.4°C)	@70°F (21.1°C)	@100°F (37.8°C)	@130°F (54.4°C)
Confining stress $\sigma_0 = 0$ psi (0 mPa)					
WST_WC2	1.76E-05	0.0427	8.5806	1729.3	12579
WST_WC24	8.89E-08	0.0025	3.9575	117.43	19188
WST_WC5	2.07E-10	0.0003	0.1336	209.27	1251.2
WST_WC6	1.72E-07	0.0070	3.4828	280.25	21145
WST_WR15	5.71E-10	0.0005	0.6300	57.648	1836.2
WST_WR2	2.37E-06	0.0190	11.631	349.07	5741.6
WST_WR23	1.20E-09	0.0001	0.4386	38.019	2837.5
WST_WR24	1.48E-07	0.0613	4.9453	238.81	18750
WST_WR4	1.57E-12	5.3E-5	0.2375	26.939	1167.8
WST_WR7	5.36E-08	0.0013	2.3512	117.07	3822.5
Confining stress $\sigma_0 = 20$ psi (2.9 mPa)					
WST_WC2	2.39E-09	0.0034	0.3307	119.72	801.81
WST_WC24	1.80E-08	0.0003	0.4466	14.671	8E+07
WST_WC5	2.79E-07	0.0002	0.1338	9.0021	3E+06
WST_WC6	2.76E-07	0.0043	0.4632	44.035	2E+06
WST_WR15	2.06E-09	0.0008	0.1756	4.1226	4621.1
WST_WR2	3.78E-06	0.0036	0.2660	25.202	2717.5
WST_WR23	1.91E-10	0.0003	0.2117	15.254	25094
WST_WR24	5.51E-08	0.0008	0.1950	43.557	21057
WST_WR4	3.02E-08	0.0003	0.1361	2.5590	472.90
WST_WR7	2.91E-10	0.0004	0.2338	13.305	75017
Confining stress $\sigma_0 = 30$ psi (4.35 mPa)					
WST_WC2	5.17E-08	0.0010	0.2613	43.637	1115.3
WST_WC24	3.91E-04	0.0019	1.4699	80.789	61954
WST_WC5	6.69E-09	0.0047	1.3149	87.459	2E+05
WST_WC6	4.89E-05	0.0650	9.0402	872.61	16633
WST_WR15	4.31E-10	0.0026	0.8467	93.292	4981.9
WST_WR2	9.35E-08	0.0026	1.0168	86.354	2909.9
WST_WR23	5.27E-09	0.0002	0.4796	54.305	2837.5
WST_WR24	2.51E-09	0.0010	0.6501	126.33	6E+06
WST_WR4	1.25E-12	3.0E-5	0.1680	27.825	971.01
WST_WR7	4.30E-10	0.0021	0.4797	117.59	2E+06

Note: WST\_WC (WesTrack Cracking Section); WST\_WR (WesTrack Rutting Section)

**TABLE 4 -- Values of  $A_0$ ,  $T_0$ (K) and  $T_S$ (°C) from Equation (2)**

<b>Mixture</b>	$A_0$	$T_0$ (K)	$T_S$ (°C)
Confining stress $\sigma_0 = 0$ psi (0 mPa)			
WST_WC2	95.94	289.98	16.98
WST_WC24	114.97	296.18	23.18
WST_WC5	129.74	302.01	29.01
WST_WC6	113.05	294.92	21.92
WST_WR15	124.58	301.38	28.38
WST_WR2	98.10	292.97	19.97
WST_WR23	124.65	301.76	28.76
WST_WR24	109.20	293.86	20.86
WST_WR4	145.41	304.33	31.33
WST_WR7	111.66	298.02	25.02
Confining stress $\sigma_0 = 20$ psi (2.9 mPa)			
WST_WC2	114.44	300.77	27.77
WST_WC24	150.22	295.23	22.23
WST_WC5	128.68	296.82	23.82
WST_WC6	124.31	294.47	21.47
WST_WR15	116.70	302.58	29.58
WST_WR2	89.62	298.43	25.43
WST_WR23	135.90	301.29	28.29
WST_WR24	115.79	298.94	25.94
WST_WR4	99.41	305.07	32.07
WST_WR7	137.85	300.44	27.44
Confining stress $\sigma_0 = 30$ psi (4.35 mPa)			
WST_WC2	104.65	300.95	27.95
WST_WC24	89.17	291.88	18.88
WST_WC5	130.77	296.24	23.24
WST_WC6	91.23	289.13	16.13
WST_WR15	127.53	299.72	26.72
WST_WR2	106.49	298.32	25.32
WST_WR23	152.64	295.81	22.81
WST_WR24	150.26	295.63	22.63
WST_WR4	146.47	304.77	31.77
WST_WR7	150.17	296.63	23.63

Note: WST\_WC (WesTrack Cracking Section); WST\_WR (WesTrack Rutting Section)

**TABLE 5 -- Values of the coefficients and exponents in Equation (3)**

<b>Mixture</b>	$A_1$	$B_1$	$A_2$	$B_2$
Confining stress $\sigma_0 = 0$ psi (0 mPa)				
WST_WC2	4885789	0.2717	4020677	0.1240
WST_WC24	4201185	0.3824	4476110	0.1272
WST_WC5	4317307	0.2901	6539619	0.1071
WST_WC6	4690443	0.3757	4357089	0.1404
WST_WR15	3720400	0.3445	5320671	0.1362
WST_WR2	4432267	0.2866	4246827	0.1060
WST_WR23	3876511	0.3667	5179212	0.1242
WST_WR24	4407584	0.3402	4186176	0.1037
WST_WR4	3916019	0.3260	5697063	0.0922
WST_WR7	4010997	0.3613	4808233	0.1204
Confining stress $\sigma_0 = 20$ psi (2.9 mPa)				
WST_WC2	4368704	0.1638	4924440	0.0970
WST_WC24	3886442	0.2071	4746965	0.1299
WST_WC5	3810473	0.2248	5530017	0.1419
WST_WC6	3898491	0.2101	4797932	0.1406
WST_WR15	3839755	0.2258	4948604	0.1167
WST_WR2	4051580	0.2142	4854067	0.1256
WST_WR23	3859662	0.2696	5733998	0.1311
WST_WR24	3732573	0.2446	6307348	0.1315
WST_WR4	3923409	0.2527	5335953	0.0954
WST_WR7	3702444	0.2165	5657348	0.1409
Confining stress $\sigma_0 = 30$ psi (4.35 mPa)				
WST_WC2	3991865	0.2105	4700157	0.1436
WST_WC24	4015736	0.2602	4886535	0.1142
WST_WC5	3823842	0.2544	4794059	0.1161
WST_WC6	3802345	0.1939	4069616	0.1570
WST_WR15	3876539	0.2183	4544094	0.1531
WST_WR2	3910521	0.2114	4532523	0.1221
WST_WR23	3645308	0.2593	4844419	0.1321
WST_WR24	3902006	0.2696	5018301	0.1194
WST_WR4	3872405	0.2380	5515970	0.1149
WST_WR7	3297151	0.2246	4878915	0.1406

Note: WST\_WC (WesTrack Cracking Section); WST\_WR (WesTrack Rutting Section)

**TABLE 6 – Performance ranking for resistance to distress at high temperatures**

<b>Binder</b>	<b>Predicted from Laboratory Measurements</b>			<b>Field-Performance Rut Depth (mm)</b>
	$T_s$	$B_1$	$B_1 / T_s$	
Confining stress $\sigma_0 = 0$ psi (0 mPa)				
WST_WC2	16.98	0.2717	0.0160	6
WST_WC24	23.18	0.3824	0.0165	22
WST_WC5	29.01	0.2901	0.0099	-
WST_WC6	21.92	0.3757	0.0171	21
WST_WR15	28.38	0.3445	0.0121	8
WST_WR2	19.97	0.2866	0.0144	6
WST_WR23	28.76	0.3667	0.0128	13
WST_WR24	20.86	0.3402	0.0163	22
WST_WR4	31.33	0.3260	0.0104	7
WST_WR7	25.02	0.3613	0.0144	36
Confining stress $\sigma_0 = 20$ psi (2.9 mPa)				
WST_WC2	27.77	0.1638	0.0059	6
WST_WC24	22.24	0.2071	0.0093	22
WST_WC5	23.82	0.2248	0.0094	-
WST_WC6	21.47	0.2101	0.0098	21
WST_WR15	29.58	0.2258	0.0076	8
WST_WR2	25.43	0.2142	0.0084	6
WST_WR23	28.29	0.2696	0.0095	13
WST_WR24	25.94	0.2446	0.0094	22
WST_WR4	32.07	0.2527	0.0079	7
WST_WR7	27.44	0.2165	0.0079	36
Confining stress $\sigma_0 = 30$ psi (4.35 mPa)				
WST_WC2	27.95	0.2105	0.0075	6
WST_WC24	18.88	0.2602	0.0138	22
WST_WC5	23.24	0.2544	0.0109	-
WST_WC6	16.13	0.1939	0.0120	21
WST_WR15	26.72	0.2183	0.0082	8
WST_WR2	25.32	0.2114	0.0083	6
WST_WR23	22.81	0.2593	0.0114	13
WST_WR24	22.63	0.2696	0.0119	22
WST_WR4	31.77	0.2380	0.0075	7
WST_WR7	23.63	0.2246	0.0095	36

Note: WST\_WC (WesTrack Cracking Section); WST\_WR (WesTrack Rutting Section)

**TABLE 7– Performance ranking for resistance to distress at intermediate temperatures**

<b>Binder</b>	<b>Predicted from Laboratory Measurements</b>			<b>Field-Performance</b>
	$T_s$	$B_1$	$B_2 * T_s$	<b>% Cracking</b>
Confining stress $\sigma_0 = 0$ psi (0 mPa)				
WST_WC2	16.98	0.1240	2.1053	7
WST_WC24	23.18	0.1272	2.9476	-
WST_WC5	29.01	0.1071	3.1065	51
WST_WC6	21.92	0.1404	3.0761	100
WST_WR15	28.38	0.1362	3.8670	-
WST_WR2	19.97	0.1060	2.1170	-
WST_WR23	28.76	0.1242	3.5723	-
WST_WR24	20.86	0.1037	2.1627	-
WST_WR4	31.33	0.0922	2.8890	-
WST_WR7	25.02	0.1204	3.0118	-
Confining stress $\sigma_0 = 20$ psi (2.9 mPa)				
WST_WC2	27.77	0.0970	2.6943	7
WST_WC24	22.24	0.1299	2.8886	-
WST_WC5	23.82	0.1419	3.3784	51
WST_WC6	21.47	0.1406	3.0191	100
WST_WR15	29.58	0.1167	3.4521	-
WST_WR2	25.43	0.1256	3.1926	-
WST_WR23	28.29	0.1312	3.7101	-
WST_WR24	25.94	0.1315	3.4114	-
WST_WR4	32.07	0.0954	3.0584	-
WST_WR7	27.44	0.1409	3.8669	-
Confining stress $\sigma_0 = 30$ psi (4.35 mPa)				
WST_WC2	27.95	0.1436	4.0120	7
WST_WC24	18.88	0.1142	2.1552	-
WST_WC5	23.24	0.1161	2.6983	51
WST_WC6	16.13	0.1570	2.5321	100
WST_WR15	26.72	0.1531	4.0898	-
WST_WR2	25.32	0.1221	3.0917	-
WST_WR23	22.81	0.1321	3.0132	-
WST_WR24	22.63	0.1194	2.7014	-
WST_WR4	31.77	0.1149	3.6498	-
WST_WR7	23.63	0.1406	3.3218	-

Note: WST\_WC (WesTrack Cracking Section); WST\_WR (WesTrack Rutting Section)

**TABLE 8 – Examples of proper choice of temperatures for triaxial modulus testing**

Binder PGxx-xx	High PG Temperature $T_{PG}(^{\circ}C)$	Choice of Five Measurement Temperatures				
		$(T_{PG}/2=)$ $T_1 (^{\circ}C)$	$(T_1-6=)$ $T_2 (^{\circ}C)$	$(T_2-6=)$ $T_3 (^{\circ}C)$	$(T_3-6=)$ $T_4 (^{\circ}C)$	$(T_4-6=)$ $T_5 (^{\circ}C)$
PG58-34	58	(58/2=) 29	(29-6=) 23	(23-6=) 17	(17-6=) 11	(11-6=) 5
PG64-22	64	(64/2=) 32	(32-6=) 26	(26-6=) 20	(20-6=) 14	(14-6=) 8
PG70-28	70	(70/2=) 35	(35-6=) 29	(29-6=) 23	(23-6=) 17	(17-6=) 11
PG82-22	82	(82/2=) 41	(41-6=) 35	(35-6=) 29	(29-6=) 23	(23-6=) 17

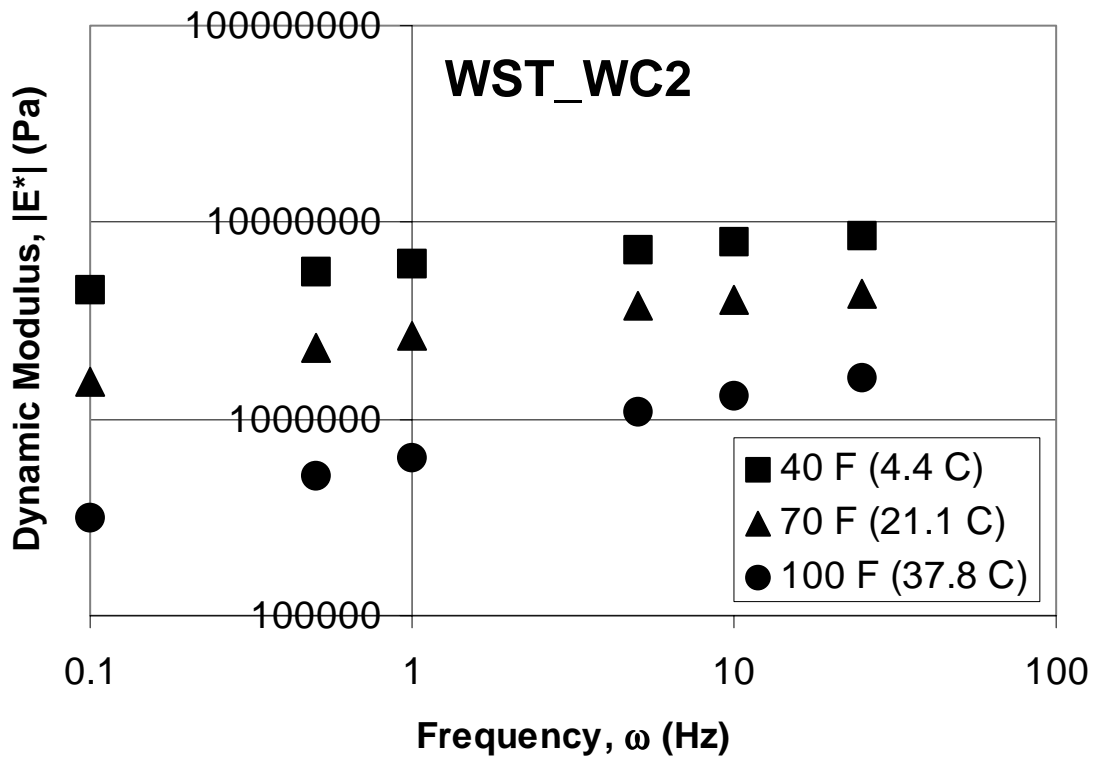


**Figure 1:** Dynamic modulus  $|E^*|$  with frequency  $\omega$  at three different temperatures of 40°F (4.4°C), 70°F (21.1°C), and 100°F (37.8°C) for WST\_WC2 laboratory-prepared samples

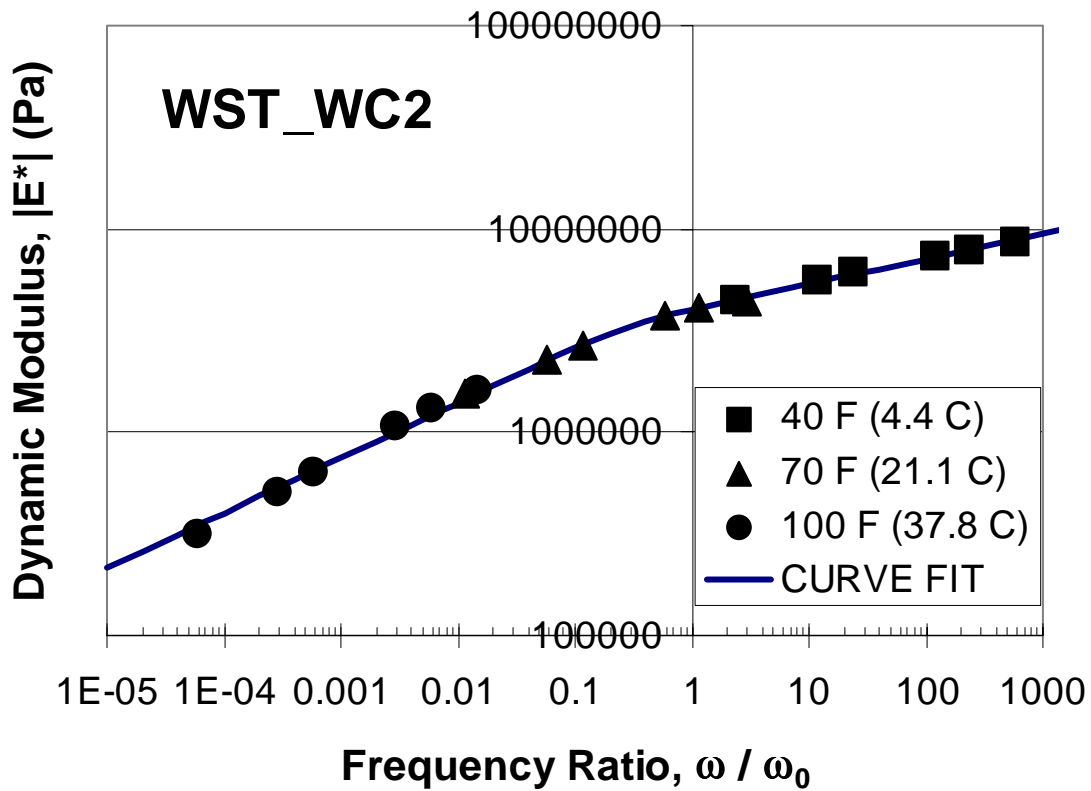


**Figure 2:** Unified curve of the dynamic modulus  $|E^*|$  with modified frequency  $\omega / \omega_0$  covering a range of 40°F (4.4°C) - 100°F (37.8°C) for WST\_WC2 laboratory-prepared samples

### Rutting Correlation for WesTrack Sections

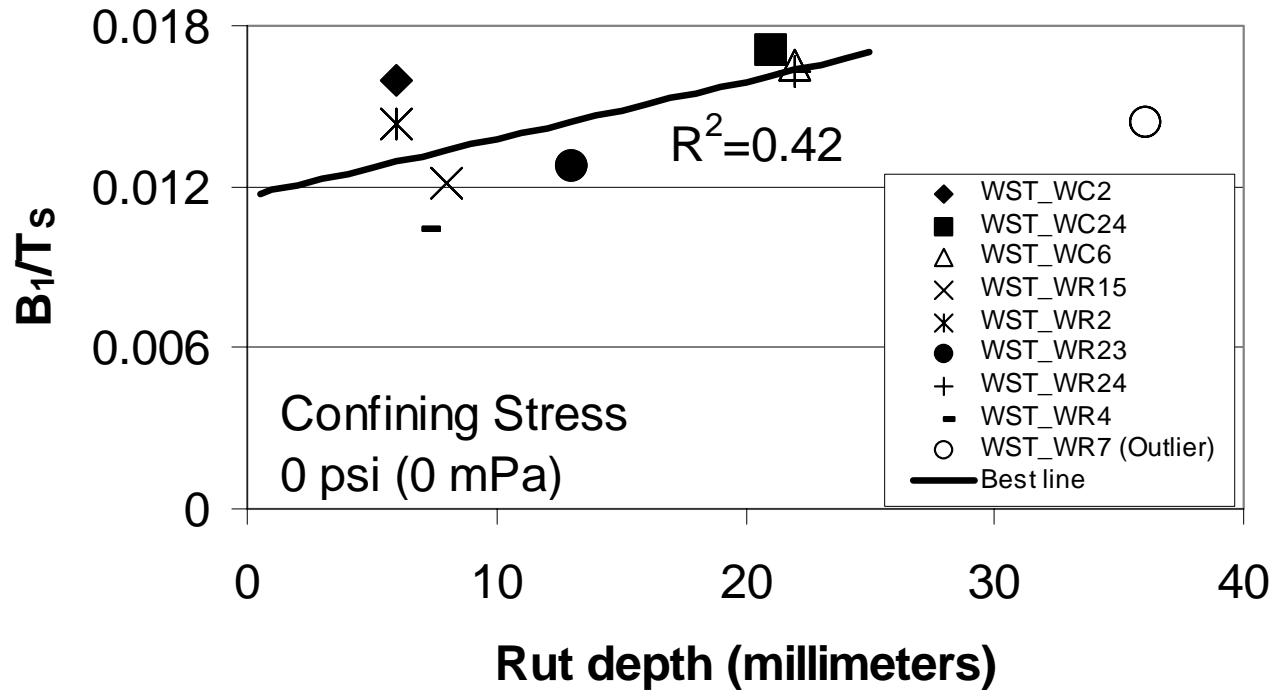


**Figure 3:** Variation of the term ( $B_1/T_s$ ) obtained from the triaxial modulus unconfined (confining stress=0psi or 0mPa) testing of laboratory-prepared samples with rut depth measurements (in millimeters) from field performance

### Rutting Correlation for WesTrack Sections

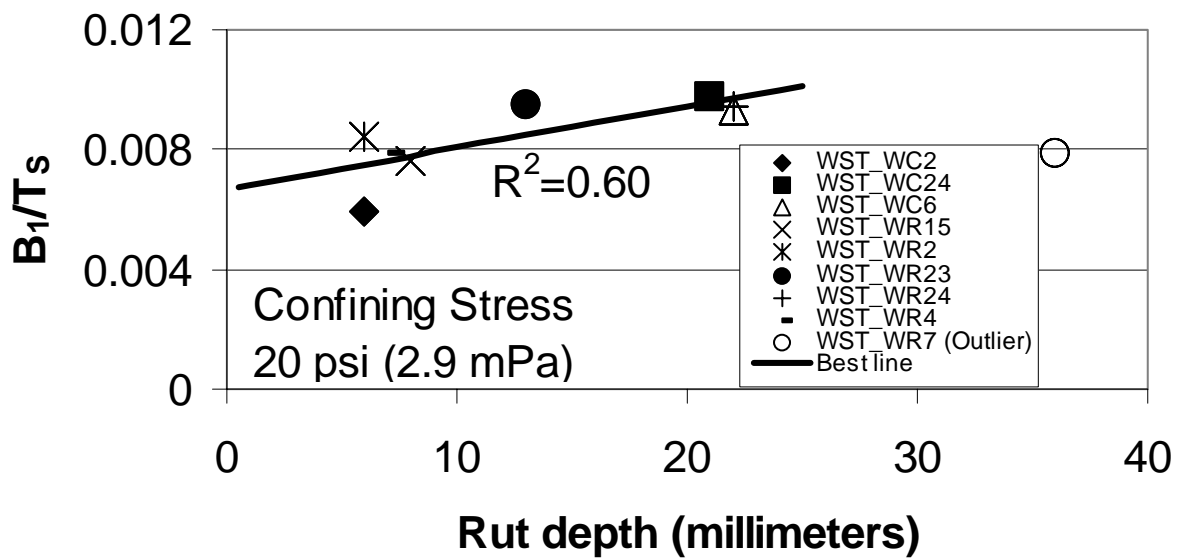


**Figure 4:** Variation of the term ( $B_1/T_s$ ) obtained from the triaxial modulus (confining stress=20psi or 2.9mPa) testing of laboratory-prepared samples with rut depth measurements (in millimeters) from field performance

### Rutting Correlation for WesTrack Sections

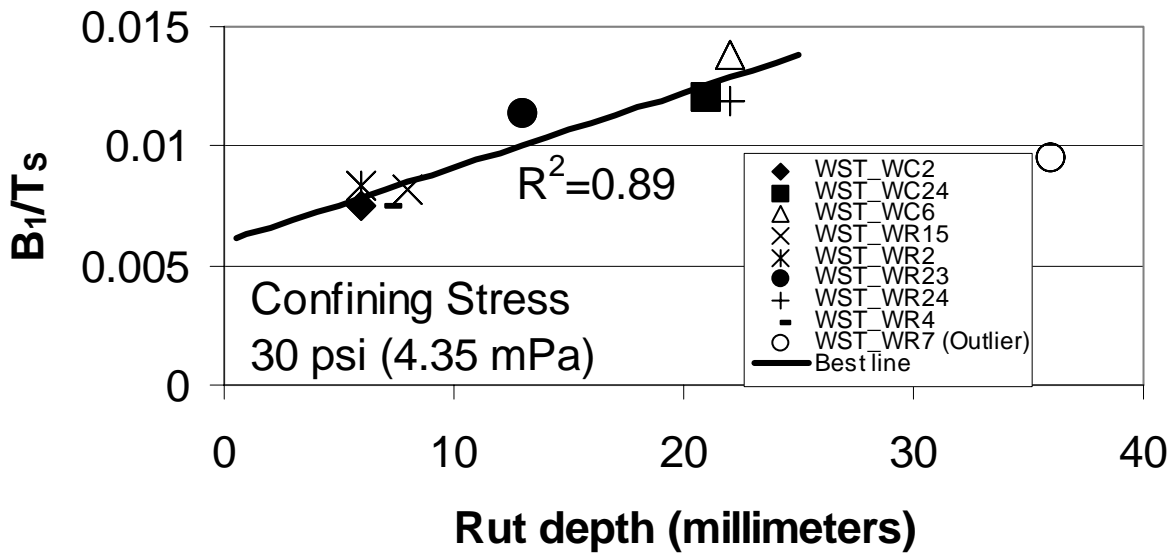


**Figure 5:** Variation of the term ( $B_1/T_s$ ) obtained from the triaxial modulus (confining stress=30psi or 4.35mPa) testing of laboratory-prepared samples with rut depth measurements (in millimeters) from field performance